International Journal of Thermophysics, Vol. 20, No. 2, 1999

Prediction of the Inversion Curve and the Maximum Value of $\mu_{J\text{-}T}$ for Some Refrigerants

E. Keshavarzi,[1] **G. Parsafar,**[1, 2] **and B. Najafi**[1]

Received July 29, 1998

In the present work, the thermodynamic states of the inversion curve have been obtained using only p–v–T data. We have also shown a linear relationship between compressibility factor and pressure for each branch of the inversion curve. These lines can be used to find the maximum inversion pressure, p_{in}^{M}. Finally, we have predicted the temperature at which the Joule–Thomson coefficient, $\mu_{J\text{-}T}$, has its maximum value for each isobar, by using the specific heat capacity, isobaric expansivity, or compressibility factor.

KEY WORDS: compressibility factor; inversion curve; Joule–Thomson coefficient.

1. INTRODUCTION

The Joule–Thomson effect is of interest not only to chemists because of its relationship to the potential function, but also to engineers for its applied aspects such as the Linde process for liquefaction of gases and its relevance to the transport of natural gases and other hydrocarbon fluids through pipelines in arctic regions [1].

The Joule–Thomson coefficient is sensitive to small deviations in temperature and pressure. Hence, it is useful for testing the applicability of an equation of state, especially the prediction of the locus of the inversion curve, which is an extremely rigorous test [2]. Nain and Aziz [3] predicted the Joule–Thomson coefficient for the noble gases at zero pressure on the basis of numerous intermolecular potentials. Edalat et al. [4] presented a

---

[1] Isfahan University of Technology, Isfahan 84154, Iran.

[2] To whom correspondence should be addressed.

0195-928X/99/0300-0651$16.00/0

correlation for the prediction of the adiabatic Joule–Thomson coefficient of pure gases and their mixtures. Colazo et al. [5] used seven cubic equations of state to predict the Joule–Thomson inversion curve for some simple fluids. Recently, Maghari and Matin [6] tested five equations of state of the van der Waals type to check their ability to predict the Joule–Thomson inversion curve.

In this work, we have calculated the inversion points from p–v–T data without fitting them with a multiparameter equation of state. We also show that the compressibility factor of each branch of the inversion curve is a linear function of pressure. And finally, we give a physical interpretation for the maximum of $\mu_{\text{J–T}}$ versus temperature for each isobar.

2. CALCULATION OF THE INVERSION POINTS USING P–v–T DATA

The Joule–Thomson inversion curve is the locus of thermodynamic states at which the temperature is invariant under isenthalpic expansion. In temperature–pressure space, the inversion curve is nearly parabolic, with a maximum inversion pressure, p_{in}^{M}, almost at an intermediate temperature. At any inversion state,

$$\mu_{\text{J–T}} = (\partial T/\partial p)_H = 0 \tag{1}$$

Using the thermodynamic relations, we may obtain

$$\mu_{\text{J–T}} = \frac{1}{C_p}\,[T(\partial v/\partial T)_p - v] \tag{2}$$

By using $Z = pv/RT$, Eq. (2) reduces to

$$\mu_{\text{J–T}} = \frac{RT^2}{pC_p}(\partial Z/\partial T)_p \tag{3}$$

As is evident from Eq. (3), at inversion points, $(\partial Z/\partial T)_p$ must be equal to zero. Therefore, if the compressibility factor is plotted versus the temperature for each isobar, the extremum points are the inversion points at which $\mu_{\text{J–T}}$ is equal to zero. One of them corresponds to the lower, and the other one to the upper, branch of the inversion curve. We have plotted such curves by using the experimental data for Ar [7] for different isobars. In Fig. 1a, Z is plotted versus T for the temperature range of 600 to 800 K at $p = 0.8$ MPa, at which we observe a maximum. A similar curve is presented in Fig. 1b for $p = 4$ MPa in a low-temperature range, where a minimum

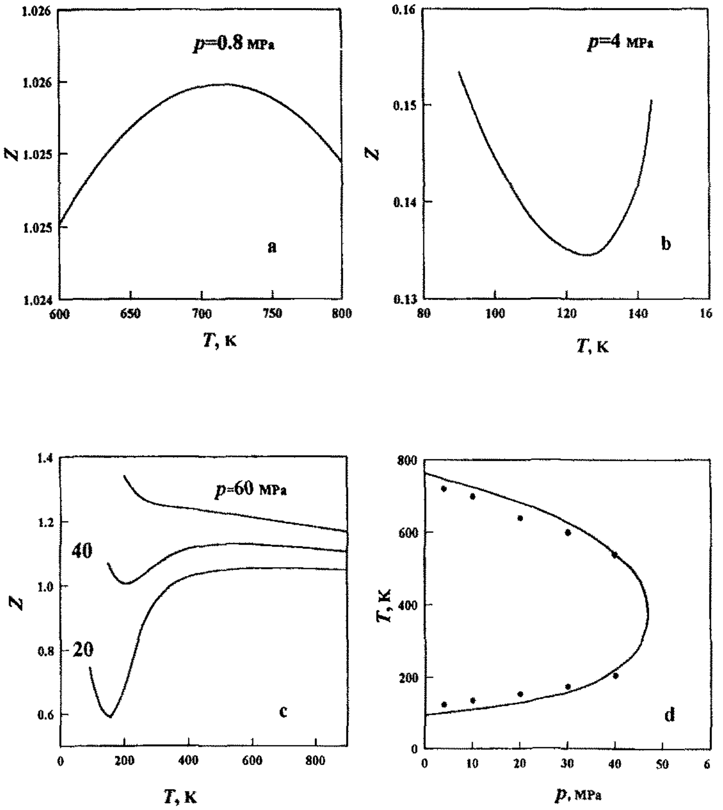

Fig. 1. Determination of the inversion points of Ar using p–v–T data [7] for different isobars. The inversion points (●) are compared with the experimental inversion curve [9] in d.

exists. These minimum and maximum points are the inversion points, and each corresponds to a point of the lower and upper branches of the inversion curve, respectively. We have also plotted such curves in the supercritical region for different pressures in Fig. 1c. At pressures below p_{in}^{M}, there are a maximum and a minimum that correspond to the upper and lower branches of the inversion curve, respectively. As the pressure increases, the maximum and minimum points approach each other until, at p_{in}^{M}, they coincide and appear as an inflection point. For this special case, both $(\partial Z/\partial T)_p$ and $(\partial^2 Z/\partial T^2)_p$ are equal to zero. For pressures above p_{in}^{M}, there is no extremum (see the top curve in Fig. 1c). In Fig. 1d, we have compared the inversion points we obtained in this way with those reported in the literature [8].

In such an investigation, we may expect that an equation of state can be used to predict the inversion curve with reasonable accuracy if the compressibility factor is at least a cubic function of temperature.

To interpret the inversion curve, let us specify the contributions of the internal and thermal pressures ($p_{\mathrm{in}}, p_{\mathrm{th}}$) to the compressibility factor separately. With $p = p_{\mathrm{th}} - p_{\mathrm{in}}$, where $p_{\mathrm{th}} = T(\partial p/\partial T)_v$ and $p_{\mathrm{in}} = (\partial E/\partial v)_T$ (E is the internal energy), the compressibility factor may be written as the algebraic sum of the thermal, Z_{th}, and internal, Z_{in}, contributions:

$$Z = \frac{p}{\rho RT} = \frac{p_{\mathrm{th}} - p_{\mathrm{in}}}{\rho RT} = Z_{\mathrm{th}} - Z_{\mathrm{in}} \tag{4}$$

where ρ is the molar density and RT has its usual meaning. Since at each inversion point, $(\partial Z/\partial T)_p = 0$, we may write

$$(\partial Z_{\mathrm{th}}/\partial T)_p = (\partial Z_{\mathrm{in}}/\partial T)_p \tag{5}$$

This means that at any inversion point, the contributions of the thermal and internal compressibility factors in $\mu_{\mathrm{J\text{-}T}}$ are equal. At the particular point on the inversion curve at which the pressure is $p_{\mathrm{in}}^{\mathrm{M}}$, in addition to the equality of $(\partial Z_{\mathrm{th}}/\partial T)_p$ with $(\partial Z_{\mathrm{in}}/\partial T)_p$, the following constraint is valid:

$$(\partial^2 Z/\partial T^2)_{p_{\mathrm{in}}^{\mathrm{M}}} = (\partial^2 Z_{\mathrm{th}}/\partial T^2)_{p_{\mathrm{in}}^{\mathrm{M}}} - (\partial^2 Z_{\mathrm{in}}/\partial T^2)_{p_{\mathrm{in}}^{\mathrm{M}}} = 0 \tag{6}$$

which indicates that $(\partial Z/\partial T)_p$ is a maximum at the temperature corresponding to $p_{\mathrm{in}}^{\mathrm{M}}$.

3. PREDICTION OF THE RELATIONS AMONG Z, p, AND T ON THE INVERSION CURVE

The compressibility factor is a function of two thermodynamic variables, such as temperature and pressure. Because of the relation between T and p on the inversion curve (the parabolic dependency of p with respect to T), it is possible to express the compressibility factor on the inversion curve in terms of only one variable, pressure or temperature. To quantify this dependency, we have used the van der Waals equation of state (vdW EOS) because of its simplicity. It is to be noted that the vdW EOS may be applied just for the upper branch of the inversion curve (low density). Using the vdW EOS, we may write Z as

$$Z = \frac{1}{1 - b\rho} - \frac{a\rho}{RT} \tag{7}$$

where a and b are the vdW constants. As we mentioned before, on the inversion curve $(\partial Z/\partial T)_p = 0$ and $\alpha = 1/T$ or $(\partial \rho/\partial T)_p = -\rho/T$, then the density of the inversion curve will depend on T as

$$\rho = \frac{1}{b} - \left(\frac{RT}{2ab}\right)^{1/2} \tag{8}$$

By substitution of ρ from Eq. (8) in Eq. (7), we may obtain the relation among Z, T, and p for the inversion states as

$$Z_{\text{in}} = \left(\sqrt{2} + \frac{1}{\sqrt{2}}\right)\left(\frac{a}{RTb}\right)^{1/2} - \frac{a}{bRT} \tag{9}$$

and

$$p_{\text{in}} = \frac{2}{b}\left(\frac{2aRT}{b}\right)^{1/2} - \frac{3RT}{2b} - \frac{a}{b^2} \tag{10}$$

To generalize the above results, Eqs. (9) and (10) may be written in the reduced forms,

$$Z = 6\sqrt{\frac{3}{T^*}} - \frac{9}{T^*} \tag{11}$$

and

$$p^* = 24\sqrt{3T^*} - 12T^* - 27 \tag{12}$$

where $p^* = p/(a/27b^2)$ and $T^* = T/(8a/27Rb)$. We solved these equations numerically and found that the compressibility factor is a linear function of pressure (Fig. 2a). To find such a relation for the lower branch (dense fluid), an EOS appropriate for a dense fluid is needed. We have used the linear isotherm regularity (LIR) [9], from which the compressibility factor is given as

$$Z = 1 + A\rho^2 + B\rho^4 \tag{13}$$

where

$$B = B_1/RT \tag{14}$$

$$A = A_2 - A_1/RT \tag{15}$$

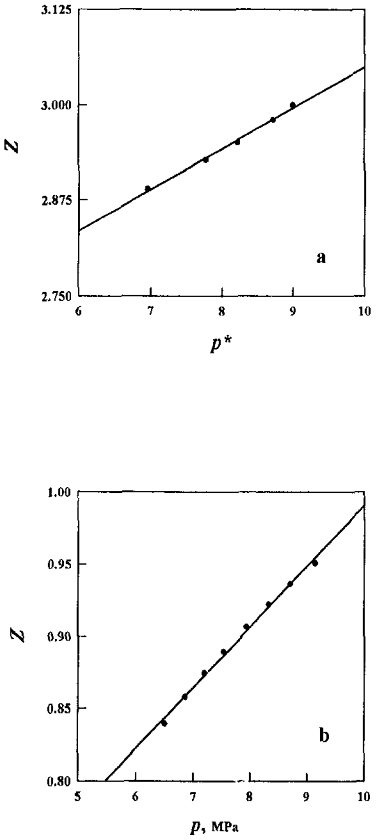

Fig. 2. The linear relationship between the compressibility factor, Z, and pressure on the inversion curve for Ar according to (a) the vdW EOS and (b) the LIR $[p^* = p/(a/27b^2)]$.

where the constants A_1 and B_1 are related to the intermolecular attraction and repulsion, respectively, and A_2 is the contribution of nonideal thermal pressure. On the inversion curve, $(\partial p/\partial T)_\rho = -\rho/T$ and the density may be written as

$$\rho = \left[\frac{3A_1 - 2A_2RT}{5B_1}\right]^{1/2} \tag{16}$$

then,

$$p = RT\left[\left(\frac{3A_1 - 2A_2RT}{5B_1}\right)^{1/2} + A\left(\frac{3A_1 - 2A_2RT}{5B_1}\right)^{3/2} + B\left(\frac{3A_1 - 2A_2RT}{5B_1}\right)^{5/2}\right] \tag{17}$$

and

$$Z = 1 + A\left[\frac{3A_1 - 2A_2RT}{5B_1}\right] + B\left[\frac{3A_1 - 2A_2RT}{5B_1}\right]^2 \tag{18}$$

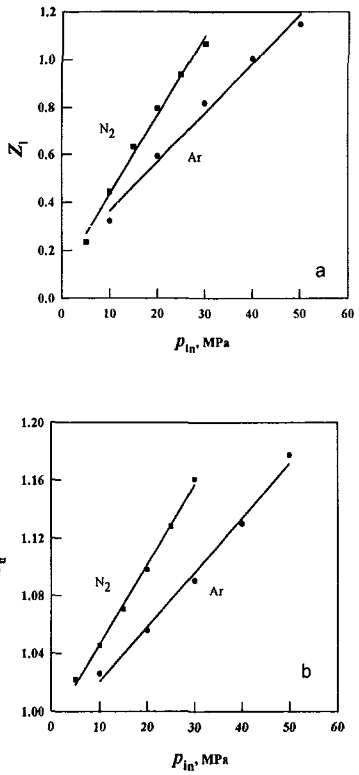

Fig. 3. The experimental linear relationship between Z and p for (a) the lower branch and (b) the upper branch of the inversion curves of Ar [7] and N_2 [10].

Table I. The Existence of a Linear Relationship Between Z and p, $Z = A + Bp$

Substance	Z	A	B (MPa^{-1})	R^2
Ar	Z_l	0.15725	0.02067	0.992
Ar	Z_u	0.98269	0.00378	0.995
N_2	Z_l	0.10386	0.03321	0.995
N_2	Z_u	0.99057	0.00554	0.998
CH_4	Z_l	0.11664	0.02252	0.991
C_2H_6	Z_l	0.08911	0.02231	0.995
CO_2	Z_l	0.06383	0.01517	0.995

We have also solved the above equations numerically for Ar [7]. As shown in Fig. 2b, Z is again linear versus p for the lower branch of the inversion curve of Ar. Figure 3 shows the experimental compressibility factor of the lower and upper branches (Z_l, Z_u) versus pressure for Ar [7] and N_2 [10]. The linear fits of the experimental data are satisfactory. Such a linearity is also observed for some other substances, for which the parameters of the lines, A (intercept), B (slope), and the coefficient of determination, R^2, are given in Table I. Such a coefficient is simply the square of the correlation coefficient [11]. The intersection point of these lines gives p_{in}^{M}. Figure 4 shows such a prediction for Ar [7].

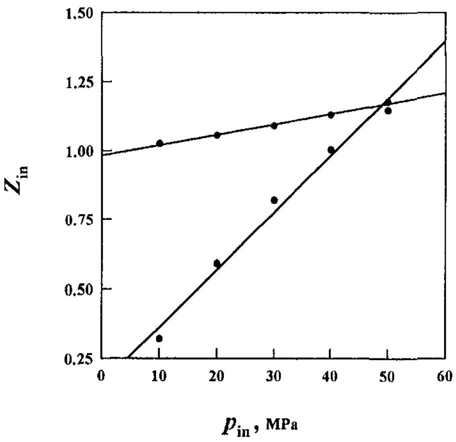

Fig. 4. Determination of the maximum inversion pressure, p_{in}^{M}, from the intersection of two lines for Ar [7] (the experimental value is about 47.5 MPa; see Ref. 8).

4. PREDICTION OF THE MAXIMUM VALUE OF $\mu_{\text{J-T}}$

The Joule–Thomson expansion is widely used for liquefaction and refrigeration of gases. Therefore, a knowledge of the Joule–Thomson coefficient of a substance at different states is very important in designing such processes.

In this section we predict the maximum value of $\mu_{\text{J-T}}$ for each isobar by using thermodynamic properties such as the specific heat, C_p, isobaric expansivity, α, and compressibility factor, Z, which are more available than the $\mu_{\text{J-T}}$.

As is well known, $\mu_{\text{J-T}}$ has a maximum value for each isobar (see Fig. 5a). If the pressure is lower than p_{in}^{M}, its maximum value is positive and located inside the parabolic inversion curve. If $\mu_{\text{J-T}}$ is plotted versus temperature at p_{in}^{M}, the maximum value of $\mu_{\text{J-T}}$ is zero and located on the inversion curve. For pressures higher than p_{in}^{M}, the value of $\mu_{\text{J-T}}$ is negative on the entire temperature range and can be ignored.

To obtain the condition at which $\mu_{\text{J-T}}$ is a maximum, we differentiate $\mu_{\text{J-T}}$, given by Eq. (3), with respect to temperature at constant pressure and set the result equal to zero to obtain

$$(\partial \mu_{\text{J-T}}/\partial T)_p = \left[\frac{2RT}{pC_p} - \frac{RT^2(\partial C_p/\partial T)_p}{pC_p^2}\right](\partial Z/\partial T)_p + \frac{RT^2}{pC_p}(\partial^2 Z/\partial T^2)_p = 0 \tag{19}$$

If $(\partial \mu_{\text{J-T}}/\partial T)_p$ is equal to zero, it is possible that both $(\partial Z/\partial T)_p$ and $(\partial^2 Z/\partial T^2)_p$ are zero. But that is true only when the pressure is equal to p_{in}^{M}, in other words, when $\mu_{\text{J-T}}^{\text{Max}}$ is located on the inversion curve ($\mu_{\text{J-T}}^{\text{Max}} = 0$). For the other isobars we have

$$\frac{RT^2(\partial C_p/\partial T)_p}{pC_p^2}(\partial Z/\partial T)_p = \frac{2RT}{pC_p}(\partial Z/\partial T)_p + \frac{RT^2}{pC_p}(\partial^2 Z/\partial T^2)_p \tag{20}$$

Therefore, when $(\partial \mu_{\text{J-T}}/\partial T)_p$ is equal to zero, none of the three terms in Eq. (19) is zero, but their sum must be zero. Even though $(\partial^2 Z/\partial T^2)_p$ is not exactly zero at the temperature at which $\mu_{\text{J-T}}$ has its maximum value, its value is very close to zero (see Fig. 5b). In other words, $(\partial Z/\partial T)_p$ has almost its maximum value when $\mu_{\text{J-T}}$ is maximum (Fig. 5b).

We conclude that we are able to predict approximately the condition at which $\mu_{\text{J-T}}$ is a maximum for each isobar using only p–v–T data. The temperature at which $(\partial Z/\partial T)_p$ is a maximum is that at which $\mu_{\text{J-T}}$ is also a maximum. This fact allows engineers, without the necessity for

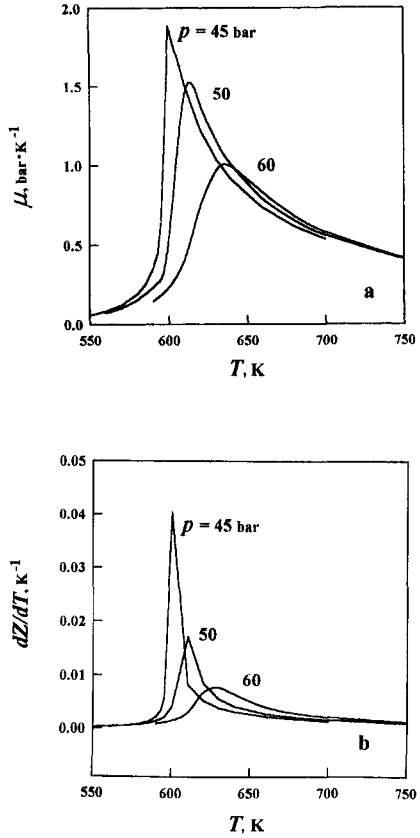

Fig. 5. (a) The Joule Thomson coefficient versus temperature for different isobars of toluene [12]. (b) Prediction of the maximum of the Joule–Thomson coefficient for each isobar using the compressibility factor data [15].

Joule–Thomson experiments, to approximate the thermodynamic location of the maximum value of $\mu_{\mathrm{J\,T}}$ in designing refrigerators.

Finally, in order to define the maximum of $\mu_{\mathrm{J\,T}}$ versus temperature in terms of the thermodynamic properties of a fluid, we may use Eq. (2) to obtain

$$\mu_{\mathrm{Max}} = \frac{T(\partial^2 v/\partial T^2)_p}{(\partial C_p/\partial T)_p} \qquad (21)$$

or

$$\mu_{\mathrm{Max}} = \frac{Tv[\alpha^2 + \alpha']}{C'_p} \tag{22}$$

where

$$\alpha' \equiv (\partial\alpha/\partial T)_p$$

and

$$C'_p \equiv (\partial C_p/\partial T)_p$$

To find the temperature at which $\mu_{\mathrm{J\text{-}T}}$ has its maximum value (for an isobar), we have to investigate the temperature dependences of α and C_p. We have used experimental data to obtain Fig. 6, for toluene [12]. As is shown, the values of both α and C_p are maxima at about the same temperature at which $\mu_{\mathrm{J\text{-}T}}$ is a maximum (but not exactly). Therefore, we may conclude that at the temperature for which $\mu_{\mathrm{J\text{-}T}}$ is a maximum for an isobar, α and C_p have almost their maximum values, and α' and C'_p are very small at such a temperature. In Table II we give predictions for the

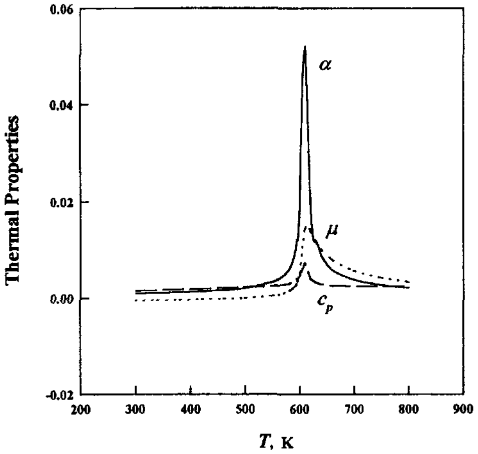

Fig. 6. The temperature dependences of α, in units of K^{-1} (solid curve), $\mu/100$, in units of $\mathrm{bar}^{-1} \cdot \mathrm{K}$ (dotted curve), and $C_p \times 10^{-5}$, in units of $\mathrm{J \cdot K^{-1} \cdot mol^{-1}}$ (dashed curve) for the 50-bar isobar of toluene [12]. Note that the maxima of all three properties are at almost the same temperature.

Table II. Prediction of the Thermodynamic State at Which μ_{J-T} Is a Maximum for Given Isobars of Some Refrigerants, Using the Experimental Isobaric Heat Capacity

Substance	p (MPa)	T (K)
R227[a]	4	390.15
R227[a]	6	413.15
R143a[b]	8	386.15
R143a[b]	10	398.15
R143a[b]	15	420.15
R32[c]	6	353.15
R32[c]	7	363.15
R32[c]	8	368.15
R32[c]	9	378.15
R32[c]	10	383.15
R32[c]	12	398.15
R32[c]	14	413.15
R152a[d]	6	403.15
R152a[d]	10	433.15

[a] From Ref. 13.
[b] From Ref. 14.
[c] From Ref. 15.
[d] From Ref. 16.

thermodynamic state at which μ_{J-T} has its maximum value for given isobars of some refrigerants, by using the experimental specific heat capacity.

5. CONCLUSION

In this work, we have calculated the inversion points from p–v–T data without fitting them to a multiparameter equation of state. The linear relationship of Z in terms of p for each branch of the inversion curve can be used to obtain the p_{in}^{M}, especially when its experimental determination is difficult or unreliable (see Fig. 4).

Finally, as mentioned previously, it is possible to predict the thermodynamic state at which the Joule–Thomson coefficient is a maximum, by investigating the temperature dependences of C_p, α,or Z (see Figs. 5 and 6). Because of the fact that the temperature dependences of such thermophysical properties are available for many fluids, whereas the experimental data for μ_{J-T} are not reported, the approach given in this paper for the prediction of μ_{J-T}^{Max} may be used in designing refrigerators.

ACKNOWLEDGMENT

We acknowledge the Iranian National Research Council for its financial support.

REFERENCES

1. K. C. Cheng and J.-W. Ou, *Can. J. Chem. Eng.* **56**:31 (1978).
2. R. D. Gune and J. M. Prausnitz, *Cryogenics* **6**:324 (1966).
3. V. P. S. Nain and R. A. Aziz, *Can. J. Chem.* **54**:2617 (1976).
4. M. Edalat, R. Bozargmehri, and J. Basiri-Parsa, *Iran. J. Chem. and Chem. Eng.* **11**:43 (1992).
5. N. V. Colazo, F. A. Silva, E. A. Muller, and C. Olivera-Fuentes, *Latin Am. Apply Res.* **22**:135 (1992).
6. A. Maghari and N. S. Matin, *J. Chem. Eng. Japan*, in press.
7. R. B. Stewart and R. T. Jacobsen, *J. Phys. Chem. Ref. Data* **18**:639 (1989).
8. R. H. Perry, D. W. Green, and J. O. Maloney, *Perry's Chemical Engineers Handbook*, 6th ed. (McGraw-Hill, New York, 1984), p. 109.
9. G. A. Parsafar and E. A. Mason, *J. Phys. Chem.* **97**:9084 (1993).
10. R. T. Jacobsen, R. B. Stewart, and M. Jahangiri, *J. Phys. Chem. Ref. Data* **15**:735 (1986).
11. J. R. Taylor, *An Introduction to Error Analysis* (University Science Books, Mill Valley, CA, 1982), p. 180.
12. R. D. Goodwin, *J. Phys. Chem. Ref. Data* **18**:1601 (1989).
13. H. Wirbser, G. Bräuning, J. Gürtner, and G. Ernst, *J. Chem. Thermodyn.* **24**:761 (1992).
14. S. L. Outcalt and M. O. McLinden, *Int. J. Thermophys.* **18**:1445 (1997).
15. R. Tillner-Roth and A. Yokozeki, *J. Phys. Chem. Ref. Data* **26**:1273 (1997).
16. S. L. Outcalt and M. O. McLinden, *J. Phys. Chem. Ref. Data* **25**:605 (1997).